Characterization of an AlGaN/GaN Electrostatically Actuated Cantilever using Finite Element Method

Nicholas DeRoller*[,1], Muhammad Qazi[1], Jie Liu[1], and Goutam Koley[1]
[1]Department of Electrical Engineering, University of South Carolina, Columbia, SC29208, USA
*Corresponding author: 301 Main St, Rm3A80, Columbia, SC29208, USA, deroller@email.sc.edu

Abstract: A 3D model of an electrostatically actuated micro cantilever has been developed for characterization using the finite element method (FEM). The microcantilever has an AlGaN/GaN HFET embedded on its base. Through various FEM simulations we are able to determine its operating frequency, electrostatic response, and strains about the AlGaN/GaN interface. This simulated cantilever system is more complex than most because it incorporates very thin subdomains. Since there is such a large difference in scale between the cantilever and the thin films, mapped and swept meshing is used heavily to reduce memory requirements and computation time. The complex, asymmetric top geometry of this structure makes 3D FEM simulation more desirable over standard PDE based analysis.

Keywords: AlGaN/GaN, FEM, HFET, microcantilever, sensor.

1. Introduction

MEMS (Micro Electro Mechanical Systems) technology has cemented its place as a mainstream technology specifically in the field of sensing applications.[1] Extensive research efforts have already been dedicated towards detecting chemicals,[2] biological molecules,[3] and explosives [4] using suspended microcantilevers. Due to its bulkiness and inability to integrate in miniaturized sensors, electrical (mostly piezoresistive and piezoelectric) transduction systems have been preferred over optical transduction for MEMS technology.

In a typical piezoresistive transduction system a piezoresistor is fabricated at the base of the cantilever where resistance is changed due to the deflection dependent strain variation.[5] This technique suffers from additional heat dissipation in the cantilever and associated thermal drifts as current flows on the cantilever. Piezoelectric materials (such as ZnO) are also difficult to integrate because they require thin film technology. Ii is challenging to achieve oriented crystal growth on metals. [6] Also, the grain structure of such materials hinders the downscaling of the devices into the nanometer range. [6]

Recently, AlGaN/GaN Heterostructure Field Effect Transistor (HFET) embedded microcantilevers have been fabricated where the HFET source drain current is shown to have significant change with cantilever bending.[7] This is because AlGaN/GaN heterostructures have large piezoelectric as well spontaneous polarization which is responsible for a highly localized 2- dimensional electron gas (2DEG) at the interface.[8] These polarization properties are dependent mostly on strain (as grown or external) created between AlGaN and GaN layers.[8][9] To accurately calculate the magnitude of HFET current while cantilever is operating in both static and dynamic mode, it is important to know the strain distribution across the whole mesa.

2. Experimental

2.1 Fabrication

250µm×50µm×2µm cantilevers were fabricated from AlGaN/GaN layers grown on Si(111) (4" wafer purchased from Nitronex Corp). 1µm i-GaN grown on 500µm thick Si substrate with 1.1µm AlN/(Al)GaN transition layer. AlGaN layer (mole fraction, x=0.26) is 17.5nm with thin 2nm GaN cap. The HFET is fabricated by common fabrication process where the mesa height was 200nm to ensure complete AlGaN down etching. Ti(20nm)/Al(100nm)/Ti(45nm)/Au(55nm) metal stack followed by rapid thermal annealing 800°C for 60s for ohmic contact formation, and Ni(25nm)/Au(375nm) Schottky gate contact patterning has been applied.[10] The GaN cantilever pattern was etched down by Inductively Coupled Plasma (ICP) Cl_2 etch (Cl_2:

32 sccm, BCl_3: 8 sccm, Ar: 5 sccm; RF_1: 70W, RF_2: 500W). Though wafer Si etch was performed by anisotropic silicon etching from the rear side ("Bosch" process).

2.2 Experimental Apparatus

Frequency response was measured using SR580 Digital Locking Amplifier from SRS. The cantilever was actuated by capacitive coupling with a microposition needle positioned within 1mm of the tip of the cantilever. The needle was fed AC signal (5V rms) by the lock-in amplifier. The oscillation of the cantilever was translated into an electrical signal using optical transduction by laser and position sensitive photo detector (PSPD).

3. Use of COMSOL Multiphysics

Figure 1(a) shows the COMSOL model of the AlGaN/GaN microcantilever (250µm×50µm ×2µm) used in this work. A 35µm by 35µm mesa is situated at the base (fixed end) of the microcantilever. The mesa is 0.2µm high with a very thin layer (17nm) of AlGaN on the top of that. The source, gate, drain, and tip metal is placed on the top of that. An extra GaN block is created at the base assigning fixed displacement to replicate the fabricated microcantilevers that hangs from a rigid body. Included in Table I are the physical properties used for AlGaN and GaN.

Table I: Properties of GaN and AlGaN used for simulation

	GaN	AlGaN
Young's Modulus (E)	210 GPa	185 GPa
Density (D)	6150 kg/m^3	5740 kg/m^3
Poisson's Ratio	0.2	0.2

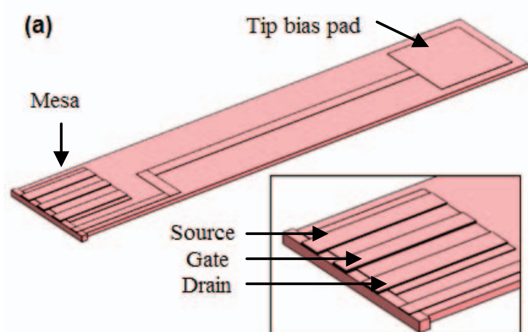

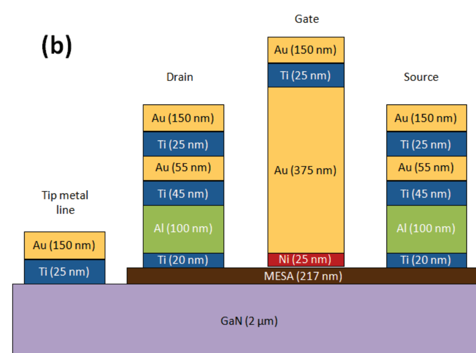

Figure 1. (a) Schematic diagram of the AlGaN/GaN microcantilever with mesa at the base. Inset shows the enlarged view of the mesa indicating source, drain, and gate contacts of the AlGaN/GaN HFET. (b) Cross section of mesa along y direction showing different metal stacks (not drawn to scale). Mesa consists of 200nm GaN and a thin 17nm AlGaN layer.

The model used contains very thin subdomains. To reduce memory requirements and processing time, mapped meshing is used over these thinly layered subdomains. The remainder of the structure is meshed using extremely fine triangular elements in the free mesher. All simulations were solved using the default Lagrange-Quadratic type elements.

Static deflection simulations were run to observe strain distributions at the AlGaN/GaN interface. For these simulations a distributed load of 0.1 nN is applied at the tip. The strain distribution output can later be used to find a strain/current relationship.

The frequency response of the AlGaN/GaN based microcantilever is simulated using harmonic analysis in COMSOL. To reduce computational time, at first we ran an eigenvalue simulation to get the first bending mode's resonant frequency. We then ran harmonic analysis in a small window around that frequency with small frequency steps. Rayleigh damping parameters were used to account for experimentally observed energy loss.

A simpler model was used for the electrostatic model due to meshing issues when an air sub domain was added. Here the 'Solid, Stress-Strain' and 'Electrostatics' modules, coupled with 'Moving Mesh', were used to solve for this dynamic problem. Maxwell stress tensors were used to couple electrostatic forces with the biasing pad located at the tip. The cantilever is placed 5µm above a 2D ground

plane and surrounded by a large enough air domain to account for fringing fields.

4. Theory

For a cantilever length L, width w, thickness t, and Young's modulus E the spring constant is given by,

$$k = \frac{Ewt^3}{4L^3} \quad (1)$$

The strain distribution along the length of the cantilever when applied a force of F at the free end is given by,

$$\varepsilon = \frac{6F(L-x)}{Ewt^2} \quad (2)$$

Where x is the length at which the strain is measured. Equation of the motion of the cantilever with effective mass *m*, and resonant frequency ω_0 is given by,[11]

$$m\frac{d^2z}{dt^2} + \left(\frac{m\omega_0}{Q}\right)\frac{dz}{dt} + kz = F(t) \quad (3)$$

Here the damping constant,

$$D = \left(\frac{m\omega_0}{Q}\right) \quad (4)$$

Moreover, Rayleigh damping model defines D as,

$$D=\alpha m+\beta k \quad (5)$$

Where, α and β are mass and stiffness damping constants.

5. Results and Discussion

5.1 Static analysis

In order to perform static analyses we applied a distributed uniform force of 0.1 nN at the free end of the microcantilever and a vertical displacement of 66.32×10^{-12} m was observed. These values give us a simulated spring constant of 1.5 N/m which is slightly larger than the theoretical valued of 1.34 N/m obtained from Eqn (1).

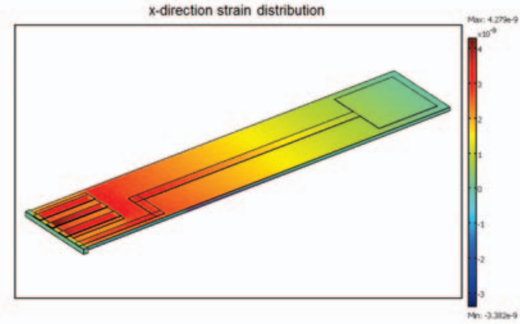

Figure 2. COMSOL simulated x-axis strain distribution shown on the surface of the microcantilever. Applied force, F=0.1 nN.

The x direction strain (ε_x) distribution on the surface is shown in Fig. 2. From Fig. 2 we can see that the highest strain is at the surface of the HFET contacts as they are at least 0.2 μm thick.

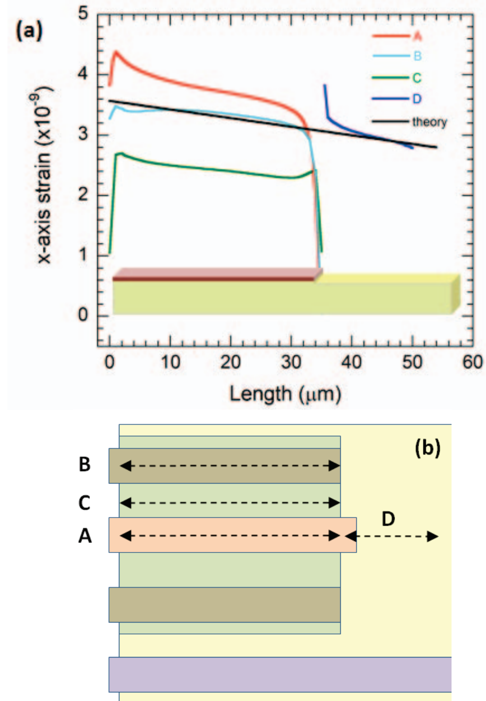

Figure 3. (a) x direction strain taken (A) on the top of the gate, (B) on the top of the source, (C) on the top of the AlGaN layer on the mesa, (D) along cantilever surface, and obtained from theoretical calculations. Inset shows a section of the cantilever including mesa for better visualization (b) the top view of the mesa showing the length along which the strain values are simulated in 3(a). Applied force, F=0.1 nN.

We found that adding extra layers on the top the base of the cantilever reduces the amount of the strain at the interface which reduces the change in HFET current per unit displacement. To investigate further the effect of metal thicknesses on the mesa we plotted the strain distribution along x-axis on the top of all contacts.

As observed from Fig. 3(a) thicker metal stacks have higher x-direction strain. For example, a gate contact with thickness of 0.575μm has the highest strain along the x-axis. Interestingly, we can see that the theoretical x-direction strain calculated from Eqn (2) almost matches with the simulated x-strain on the cantilever surface outside the mesa [see Fig. 3(a)]. Nevertheless to get a relation between the strain and HFET source drain current it is important to know the piezoelectric polarization at the interface of AlGaN and GaN layer. As described in Ref. [9], the 2DEG formation depends upon both x-strain as well the y-strain as described below by piezoelectric polarization,[9]

$$P_{PE} = e_{33}\varepsilon_z + e_{31}\left(\varepsilon_x + \varepsilon_y\right) \qquad (6)$$

Where, ε_x,ε_y, and ε_z are the x, y, and z-direction strains. And e_{33} and e_{31} are piezoelectric constants for $Al_xGa_{1-x}N$. Though it is most likely that the y and z-direction strains in the mesa region will be negligible as the base of the cantilever is fixed, we extracted the x and y-direction strains to compare the difference.

As seen from Fig. 4, on an average the y-direction strain is at least an order less that x-direction, so for source drain current simulation the y-direction strain term in Eqn. (6) can be safely ignored without much loss of accuracy.

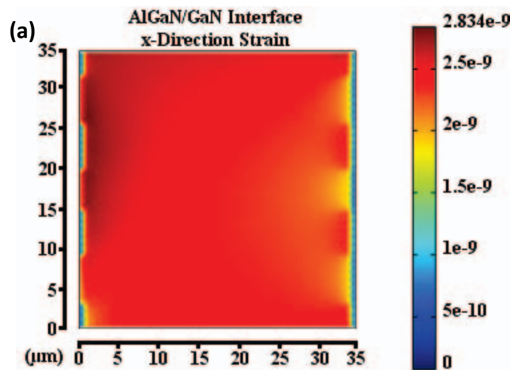

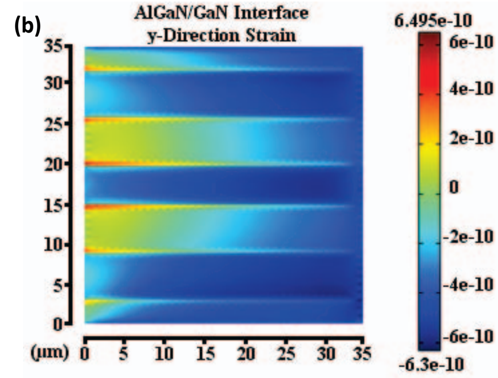

Figure 4. 2D maps of the x (a) and y-direction (b) strains at the AlGaN/GaN interface in the mesa region with the application of 0.1 nN force.

Another important factor in determining the piezoelectric polarization is the variation of x-strain along the vertical direction. For as-grown AlGaN/GaN systems, the polarization is spatially uniform in either AlGaN or GaN; the difference in polarization occurs only at the interface. For microcantilever bending, the strain is in x-direction whereas the displacement of the cantilever is in z-direction. Therefore, the x-strain distribution is supposed to vary spatially inside these materials.

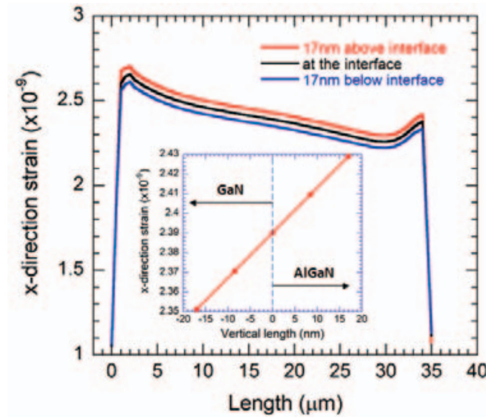

Figure 5. x-direction strain at the AlGaN/GaN interface, 17nm above and below the interface. Inset shows the x-direction strain variation along the vertical direction.

As seen from Fig. 5, the x strain along the length of the mesa is different when extracted from 17nm above and below the interface. Inset of Fig. 5 shows that this change follows an approximate linear relation. Obviously, these strain variations create a polarization profile that

will not change abruptly at the interface. It is expected that the 2DEG at the AlGaN/GaN interface will spread out into GaN. We are currently investigating this effect.

5.2 Harmonic Analysis

Both experimental and simulated frequency sweeps are shown in Fig. 6 where the experimental data done in air is rescaled to have a better comparison with the simulated one. There is a shift in the frequencies where the peaks are greatest. This may be due to over etch of the microcantilevers during fabrication. It is a complicated task to model the damping parameters in such systems, because we calculated β from experimentally obtained quality factor Q. Putting effecting mass of 37.31 pg and ω_0=193.6 rad/s we obtain $\beta=5.94\times10^{-8}$. α is assumed zero by default. We added this value to COMSOL and ran the harmonic analyses. However, we found the simulated Q to be 50.5, which is lower than the experimental value.

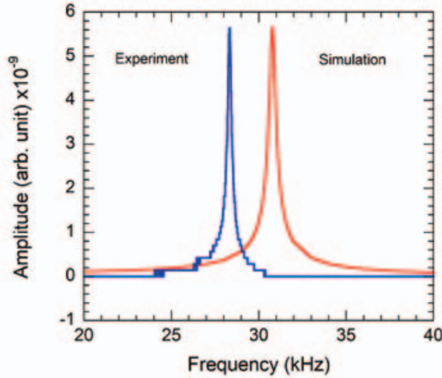

Figure 6. Experimental and simulated frequency sweep for the AlGaN/GaN microcantilever. $f_{s,sim}$=30.8 kHz and Q_{sim}=50.5; $f_{s,exp}$=28.3 kHz and Q_{exp}=80.

5.3 Electrostatic Analysis

Transient analyses were performed to simulate a capacitive coupled cantilever with a ground electrode as reference. The cantilever tip is excited with a sinusoidal voltage. The oscillation depends on quality factor (Q), ac voltage (V_{ac}), surface work function difference between cantilever and ground electrode (Δφ), spring constant (k), cantilever and ground separation (z), area of the tip metal (A), and the relative permittivity of the medium in between (ε).[12] This is shown in:

$$\Delta a=\left(\frac{\varepsilon \mathrm{A}}{\mathrm{z}^2}\cdot\frac{Q}{k}\cdot \mathrm{V}_{\mathrm{ac}}\right)\times\Delta\varphi \qquad (7)$$

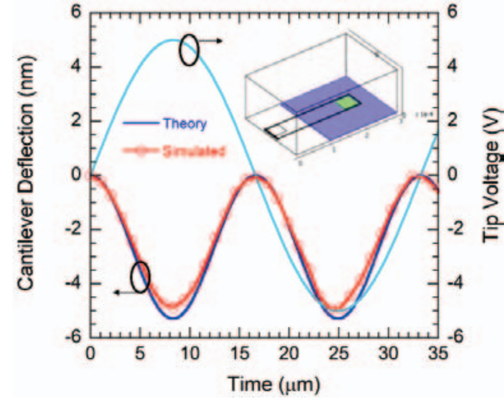

Figure 7. Theoretical and simulated (COMSOL) time dependent cantilever deflection in air with the application of $5\sin(\omega_0 t)$ on the tip metal. Tip to ground separation was 5μm and the tip metal area, A=40μm×40μm. Quality factor, Q=80. Inset shows the model used to simulation.

Theoretical calculation was done (see Fig. 7) for time dependent deflection of the cantilever by solving Eqn. (3) using ode45 of MATLAB. ode45 uses a variable step Runge-Kutta method to solve ordinary differential equations. We are unable to run an electrostatic transient simulation where ac coupled displacement is desired. This is because COMSOL takes the ac signal as discrete dc voltages sampled over time and then does an electrostatic solution at each sample. Therefore the simulated displacement does not incorporate Q as shown in Eqn. 7. To handle this case, we considered Q=1 in the Eqn. (3) to facilitate direct comparison between the theory and COMSOL simulation. As seen from Fig. 7, there is a slight discrepancy between the theoretical and simulated values. This is due to the ability of COMSOL to simulate the fringing effect and to incorporate the non-uniformity of the tip and ground metal separation.

6. Conclusion

AlGaN/GaN cantilevers have been built and simulated for use as resonant microsensors. Because the strains about the HFET are important for source and drain current calculation we examined how structures such as the metal stacks affected the strain distribution. x

and y-strain distributions were extracted; we found that y-strain is an order lower than x-strain, therefore it can safely be ignored for faster computation. We also observed the dependence of x-strain on vertical distance inside mesa which is expected to spread the 2DEG inside GaN. In harmonic analysis, Rayleigh damping parameter was calculated from experimental quality factor in an attempt to find out quality factor from simulated frequency sweep. It is shown in these simulations that modeling thinly layered features using FEM software such as COMSOL gives several advantages over standard PDE based analysis.

7. References

1. V. Cimalla, J. Pezoldt, and O. Ambacher, Group III nitride and SiC based MEMS and NEMS: materials properties, technology and applications, *J. Phys. D*, **40**, 6386-6434 (2007).
2. Z. Hu, Z, T. Thundat, R. J. Warmack, Investigation of adsorption and absorption-induced stresses using microcantilever sensors. *J. Appl. Phys.*, **90**, 427-431 (2001).
3. T. P. Burg1, M. Godin, S. M. Knudsen, W. Shen, G. Carlson, J. S. Foster, K. Babcock, and S. R. Manalis, Weighing of biomolecules, single cells and single nanoparticles in fluid, *Nature*, 446, 1066-1069 (2007).
4. L. A.Pinnaduwage, A. Gehl, D. L. Hedden, G. Muralidharan, T. Thundat, R. T. Lareau, T. Sulchek, L. Manning, B. Rogers, M. Jones, J. D. Adams, A microsensor for trinitrotoluene vapor. *Nature*, **425**, 474 (2003).
5. N. V. Lavrik, M. J. Sepaniak, and P. G. Datskos, Cantilever transducers as a platform for chemical and biological sensors, *Rev. of Scientific Instruments*, **75**, 2229-2253 (2004).
6. K. Tonisch,C. Buchheim, F. Niebelschütz, A. Schober, G. Gobsch, V. Cimalla, O. Ambacher, and R. Goldhahn, Piezoelectric actuation of (GaN/)AlGaN/GaN heterostructures, *J. Appl. Phys.,* **104**, 084516 (2008).
7. T. Zimmermann, M. Neuburger, P. Benkart, F. J. Hernández-Guillén, C. Pietzka, M. Kunze, I. Daumiller, A. Dadgar, A. Krost, and E. Kohn, “Piezoelectric GaN Sensor Structures”, *IEEE Electro. Device Lett.*, **27**, 309 (2006)
8. T. Zimmermann et. al., "Piezoelectric GaN Sensor Structures", IEEE Electro. Device Lett. **27**, 309 (2006).
9. O. Ambacher et. al., “Two-dimensional electron gases induced by spontaneous and piezoelectric polarization charges in N- and Ga-face AlGaN/GaN heterostructures”, *J. Appl. Phys.*, **85**, 3222 (1999).
10. M. Eickhoff, et. al., “Piezoresistivity of AlxGa1-xN layers and AlxGa1-xN/GaN heterostructures”, *J. Appl. Phys.*, **90**, 3383 (2001).
11. N. Sasaki, and M. Tsukada, “The relation between resonance curves and tip-surface interaction potential in noncontact atomic-force microscopy”, *Jap. J. Appl. Phys.*, **35**, L533 (1998).
12. G. Koley et. al., “Gas sensing using electrostatic force potentiometry,” *Appl. Phys. Lett*. **90**, 173105 (2007).

8. Acknowledgements

We thankfully acknowledge financial support from National Science Foundation (NSF) Grant No. ECCS-0801435, and Army Research Office Grant No. W911NF-08-0299.